tischen Zusammenstellung als wahrscheinlichsten Wert 3608,0 XE. an, während alle Bestimmungen aus den folgenden Jahren etwas niederere Werte, 3607,5 bis 3607,1 XE. liefern. Die Unterschiede sind grösser, als dass sie durch Verschiedenheiten des Brechungseinflusses erklärt werden könnten. Am sichersten dürfte der van Bergen'sche Wert sein, der aus Messungen an einem Einkristall erhalten wurde. Die eigenen Ergebnisse kommen diesem Wert sehr nahe.

Der Absolutwert jeder Gitterkonstantenmessung ist noch mit dem Fehler der Wellenlängenmessung behaftet. Die Angabe der Wellenlänge für Ni–$K\alpha_1$-Strahlung (Eriksson, 1928) mit 1654,50 XE. ist genau auf $\pm$0,012 XE. Dies bedeutet für die Gitterkonstante von Kupfer ein $\Delta a = \pm 0{,}026$ XE. Dieser Umstand ist zu berücksichtigen, wenn Gitterkonstanten, die mit verschiedenen Strahlungen bestimmt wurden, miteinander verglichen werden sollen. Zusammenfassend ist zu sagen, dass bei Angabe der Gitterkonstanten von Kupfer in XE. schon die erste Stelle hinter dem Komma nicht mehr ganz sicher ist.

Zusammenfassung

1. Eine bei Chrom und Kupfer beobachtete Häufigkeitsverteilung der Gitterkonstante verschwindet, wenn die Metalle im Hochvakuum bei Temperaturen in der Nähe des Schmelzpunktes entgast werden.

2. Infolge der 'natürlichen Spektrallinienbreite' kann nur der Reflexionswinkelbereich bis etwa 88½° zur Messung ausgenützt werden; experimentell wären Interferenzen bis 89½° beobachtbar.

3. Der Einfluss der Brechungskorrektion auf die Genauigkeit einer Gitterkonstantenbestimmung an Vielkristallen wird untersucht und festgestellt, dass die durch den Brechungseffekt bedingte Unsicherheit grösser sein kann als der eigentliche Versuchsfehler.

Der Deutschen Forschungsgemeinschaft sind wir für die Unterstützung der Arbeiten zu Dank verpflichtet. Herrn Prof. Dr P. P. Ewald danken wir für anregende Diskussionsbemerkungen.

References

Barrett, C. S. & Kaiser, H. F. (1931). *Phys. Rev.* **37**, 1696.
Bergen, H. van (1938). *Ann. Phys., Lpz.* **33**, 737.
Bragg, W. L. & Lipson, H. (1938). *Nature, Lond.* **141**, 367.
Compton, A. H. & Allison, S. K. (1935). *X-ray in Theory and Experiment*, 2. Aufl. New York: Van Nostrand.
Crussard, C. & Aubertin, F. (1948). *Rev. Métall.* **45**, 402.
Darwin, C. G. (1914). *Phil. Mag.* (6), **27**, 315.
Eriksson, S. (1928). *Z. Phys.* **48**, 360.
Ewald, P. P. (1917). *Ann. Phys., Lpz.* **54**, 519.
Ewald, P. P. (1920). *Z. Phys.* **2**, 332.
Ewald, P. P. (1924). *Z. Phys.* **30**, 1.
Frohnmeyer, G. (1951). *Z. Naturforsch.* **6a**, 319.
Frohnmeyer, G. & Glocker, R. (1951). *Naturwissenschaften*, **38**, 155.
Hendus, H. & Novotny, H. (1948). *Naturwissenschaften*, **35**, 61.
Hendus, H. (1950). *Bull. Soc. franç. Minér.* **73**, 187.
Hume-Rothery, W., Lewin, G. F. & Reynolds, P. W. (1936). *Proc. Roy. Soc.* A, **157**, 167.
Möller, K. (1937). *Z. Krystallogr.* **97**, 170.
Neuburger, M. C. (1936). *Z. Krystallogr.* **93**, 1.
Obinata, J. & Wassermann, G. (1933). *Naturwissenschaften*, **21**, 382.
Owen, E. A. & Yates, E. L. (1933). *Phil. Mag.* (7), **15**, 472.
Prins, J. A. (1930). *Z. Phys.* **63**, 477.
Renninger, M. (1934). *Z. Krystallogr.* **89**, 344.
Rusterholz, A. (1933). *Z. Phys.* **82**, 538.
Stenström, W. (1919). Dissertation, Lund.
Straumanis, M. & Mellis, V. (1935). *Z. Phys.* **94**, 184.

Acta Cryst. (1953). **6**, 24

The Crystal Structure of Datolite

By T. Ito and H. Mori
Mineralogical Institute, University of Tokyo, Japan

(*Received* 7 *May* 1952)

The structure of datolite has been analysed by means of the two-dimensional Fourier syntheses supplemented by a (linear) three-dimensional synthesis, using oscillation and Weissenberg photographs. The unit cell has the dimensions $a = 4{\cdot}84$, $b = 7{\cdot}60$, $c = 9{\cdot}62$ Å, $\beta = 90°\ 09'$, and contains 4 $HCaBSiO_5$. The space group is $P2_1/c$. The structure, obtained by deciphering a Patterson projection, includes separate SiO_4 groups but may be described as superimposed sheets of linked O and O–OH tetrahedra around Si and B atoms held together by Ca atoms. It is pointed out that the structure of gadolinite can be derived from that of datolite by simple replacement of atoms.

Introduction

Datolite, together with gadolinite and homilite, forms a well-defined group of minerals whose structural type is yet to be determined. This group was once regarded as including also euclase (Bragg, 1937, p. 162). However, although their space groups are the same, the lattice dimensions and cleavage of euclase and datolite differ considerably and we cannot deduce between

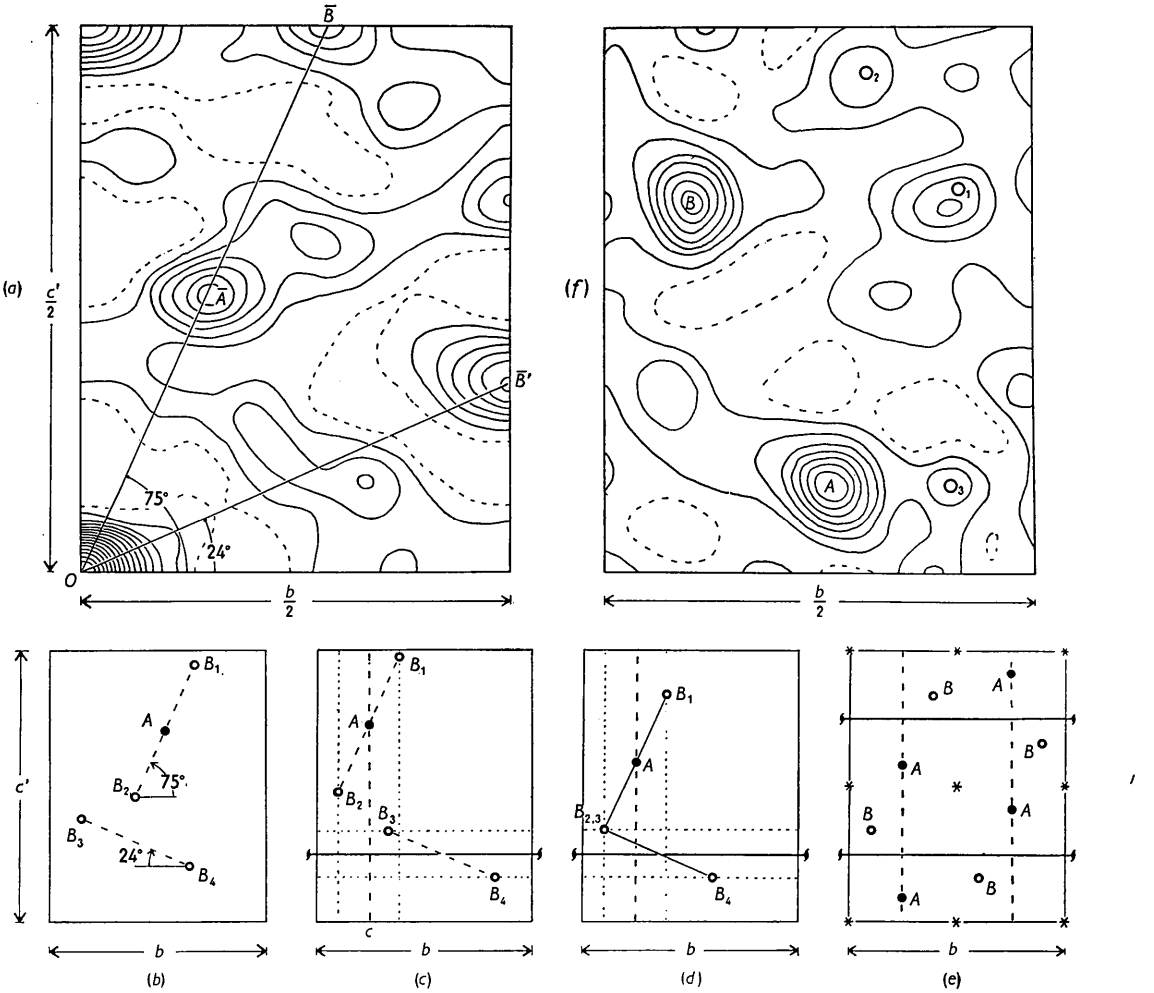

Fig. 1. Course of analysis illustrated. (*a*) Patterson projection on (100)′. (*b*)–(*e*) Steps to decipher (*a*) (see text, symmetry symbols as usual). (*f*) Fourier projection on (100)′ (first synthesis).

them any reasonable relationship such as might be expected between kindred structures. The present study was undertaken to clarify the position of the datolite group in relation to euclase and other silicates.

Experimental

The specimens used in the study are short prismatic crystals from Bergen Hill, New Jersey, U.S.A. (Dana, 1900) having the typical composition of datolite, $HCaBSiO_5$. They were kindly supplied by K. Sakurai.

Throughout the experiments, in which oscillation and Weissenberg photographs were taken, Mo or Cu $K\alpha$ radiations were employed. Intensities were estimated visually by means of the multiple-photographic technique, giving numerical values on an arbitrary scale. Only the Lorentz and polarization factors were taken into consideration.

The unit cell and space group

The unit cell has the dimensions

$a = 4{\cdot}84 \pm 0{\cdot}005$, $b = 7{\cdot}60 \pm 0{\cdot}01$, $c = 9{\cdot}62 \pm 0{\cdot}01$ Å (oscillation photographs, $\lambda = 0{\cdot}710$ Å), $\beta = 90° 09'$ (Dana, 1900, p. 504, morphological), and contains four molecules of $HCaBSiO_5$. (We have also measured β on the Weissenberg photographs to be 90° within the experimental error.) The space group is C_{2h}^5–$P2_1/c$. These observations are in agreement with the results obtained by Gossner & Mussgnug (1929) except that a and c are interchanged to conform to the axial ratio usually adopted.

Analysis

In the yz projection of the vector cell (Fig. 1(*a*)) we read at once that $O\overline{A} = \frac{1}{2}O\overline{B}$. This indicates that, in the corresponding projection of the atom cell (Fig. 1(*b*)), a heavy atom (say A) lies halfway between two other heavy atoms (say B_1, B_2). The length and orientation of B_1–B_2 are such that the two B's are equivalent and subject to the glide plane c. The atom A must therefore lie on it (Fig. 1(*c*)).

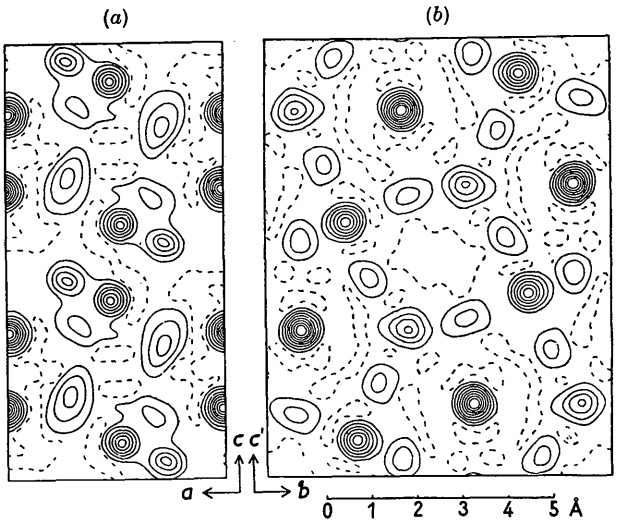

Fig. 2. Fourier projections of electron density on (*a*) (010) and (*b*) (100)′. Contours at intervals of 4 e.Å^{-2}, the zero-electron lines being broken.

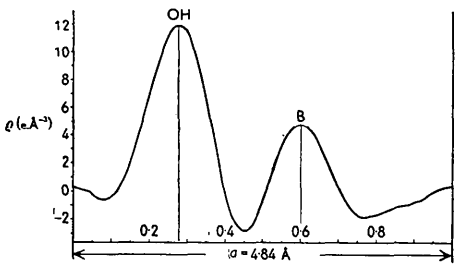

Fig. 3. Electron density along OH–B.

On the other hand, another pair of heavy atoms (say B_3, B_4; see Fig. 1(*b*)), corresponding to the vector $O\bar{B}'$ in the projected vector cell (see Fig. 1(*a*)), are again related to each other by a digonal screw axis (see Fig. 1(*c*)).

With these two restrictions simultaneously imposed, we may place B_2 and B_3 at the same point, as shown in Fig. 1(*d*). A complete set of four A's and four B's are then produced, as required by symmetry (Fig. 1(*e*)).

Since the major maxima of the vector map were satisfactorily accounted for by this distribution of heavy atoms we assumed that it represented a substantially correct picture of the structure. Silicon atoms were placed at A and calcium atoms at B, and F_{0kl}'s were calculated. The first Fourier summation was carried out using 30 experimental F_{0kl}'s* with the signs thus derived. (All these signs were subsequently proved to be correct.)

The result of the preliminary synthesis (Fig. 1(*f*)) indicated the positions of three oxygen atoms, in addition to those of calcium and silicon. The second summation was performed with 55 and the third with 95 terms. As refinement proceeded more peaks emerged in the electron-density map and we were able to read off from the fourth and final synthesis the y and z coordinates of all the atoms in the cell.

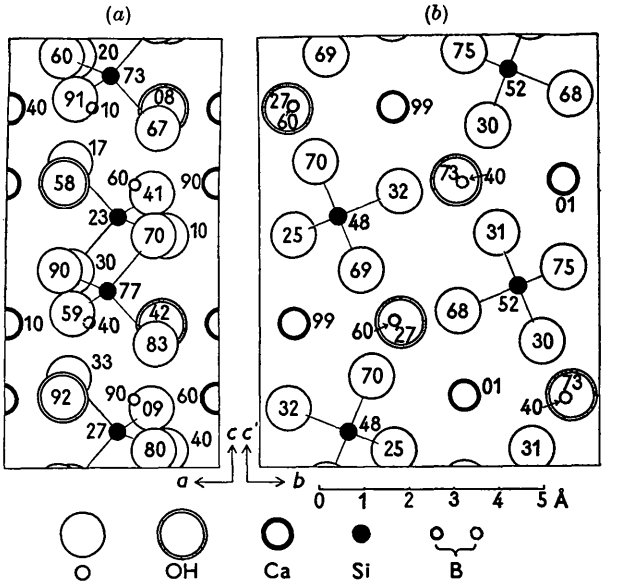

Fig. 4. The structure of datolite, projected on (*a*) (010) and (*b*) (100)′ (the figure corresponds to Fig. 2). Numbers give the height of each atom in the cell expressed as a percentage of the b and a translations.

In determining the remaining x coordinates the usual crystal-chemical concepts were utilized. The very short a length facilitated the location of atomic sites. The final decision, however, was reached after the completion of an xz Fourier synthesis, using experimental F_{h0l}'s*. Even this could not eliminate ambiguity as to the x coordinate of boron since it is overlapped by an oxygen atom in this projection. A three-dimensional summation along [100] passing the OH group and an boron atom was therefore resorted to:

$$\varrho_{x,y,z} = \frac{1}{V} \sum^{k} \sum^{h} \sum^{l} F_{hkl} \cos 2\pi (hx/a + ky/b + lz/c),$$

where we put $y/b = 0{\cdot}400$, $z/c = 0{\cdot}340$.

The number of terms used was 668, F's with $4 \sin^2 \theta/\lambda^2 > 1{\cdot}50$ Å^{-2} being cut off. The a length was subdivided into 60 parts, giving intervals of 0·08 Å. For the summation F's were multiplied by the tem-

Table 1. *Coordinates of atoms*

Atom	No. of equivalent atoms in the cell	x/a	y/b	z/c
Si	4	0·475	0·265	0·083
Ca	4	0·990	0·103	0·338
B	4	0·600*	0·400	0·340
O(1)	4	0·25	0·395	0·040
O(2)	4	0·69	0·300	0·460
O(3)	4	0·70	0·330	0·210
O(4)	4	0·32	0·085	0·140
OH	4	0·275*	0·415	0·335

* Results of the three-dimensional summation. The xz synthesis gave $x_B = 0{\cdot}60$, $x_{OH} = 0{\cdot}28$.

* Multiplied by the temperature factor, $\exp[-B(\sin\theta/\lambda)^2]$ with $B = 0{\cdot}5$ Å^2.

Table 2. *Observed and calculated F's*

(*a*) Weissenberg photographs (Cu $K\alpha$)

hkl	F_o	F_c
002	10	− 8
004	58	−55
006	47	41
008	33	−31
0,0,10	24	−26
0,0,12	36	32
011	23	−15
012	3	− 5
013	8	− 2
014	52	−44
015	18	−16
016	4	− 6
017	9	6
018	53	57
019	7	12
0,1,10	5	− 4
0,1,11	9	− 6
020	25	−30
021	6	− 7
022	42	−38
023	9	5
024	13	−16
025	70	65
026	58	50
027	5	− 6
028	14	13
029	7	−11
0,2,10	15	−22
0,2,11	11	24
031	12	17
032	62	65
033	31	−34
034	40	−40
035	12	12
036	16	−16
037	8	− 7
038	—	2
039	—	− 3
0,3,10	51	−47
0,3,11	11	6
040	48	−54
041	34	−38
042	38	38
043	11	−15
044	13	12
045	—	0
046	59	−66
047	—	− 7
048	—	2
049	6	1
0,4,10	40	34
051	14	15
052	14	−22
053	10	8
054	19	−22
055	19	20
056	14	14
057	12	17
058	9	10
059	27	−26

hkl	F_o	F_c
060	58	−64
061	30	29
062	4	− 4
063	13	16
064	31	41
065	10	−12
066	15	−13
067	12	12
068	9	9
069	10	− 4
071	—	− 2
072	12	−14
073	10	6
074	59	58
075	14	−15
076	6	6
077	12	−12
080	20	22
081	19	12
082	2	5
083	19	−18
084	10	−16
085	19	−24
086	—	− 1
091	17	−24
092	14	−21
093	10	16
100	20	−22
200	7	1
300	71	60
400	83	71
500	4	− 4
600	31	29
102	66	−72
202	6	13
302	72	−63
402	10	3
502	41	−32
104	66	−63
204	19	−26
304	13	11
404	32	−21
504	27	−26
106	66	62
206	10	−12
306	78	74
406	30	17
506	36	31
108	19	−23
208	—	− 2
308	—	7
408	47	−42
1,0,10	27	−35
2,0,10	—	5
3,0,10	16	−18
$10\bar{2}$	12	−16

hkl	F_o	F_c
$20\bar{2}$	34	−36
$30\bar{2}$	10	− 9
$40\bar{2}$	13	− 6
$50\bar{2}$	9	− 4
$10\bar{4}$	63	64
$20\bar{4}$	78	−71
$30\bar{4}$	21	−36
$40\bar{4}$	38	−24
$50\bar{4}$	—	2
$10\bar{6}$	70	62
$20\bar{6}$	4	8
$30\bar{6}$	45	54
$40\bar{6}$	13	12
$50\bar{6}$	48	38
$10\bar{8}$	22	22
$20\bar{8}$	17	−17
$30\bar{8}$	10	− 9
$40\bar{8}$	9	2
$1,0,\bar{10}$	18	−20
$2,0,\bar{10}$	9	− 1
$3,0,\bar{10}$	42	−48
110	2	− 2
120	63	57
130	66	−59
140	73	−60
150	21	−20
160	—	2
170	25	25
180	9	3
210	8	− 4
220	15	−19
230	7	10
240	12	13
250	16	16
260	29	−32
270	17	−14
280	31	34
310	7	− 2
320	24	30
330	49	50
340	53	−61
350	—	− 4
360	—	− 6
370	8	14
380	—	− 5
410	38	−27
420	9	−10
430	35	−27
440	35	−17
450	8	− 1
460	38	−35
510	34	−17
520	31	26
530	26	14
540	34	−30
550	8	−10

Table 2 (*cont.*)

(*b*) Oscillation photographs (Mo $K\alpha$)

hkl	F_o	F_c
111	46	−44
112	52	56
113	63	64
114	14	24
115	9	−10
116	8	− 7
117	15	−19
118	14	−12
119	30	28
1,1,10	23	−24
1,1,11	—	− 4
121	58	−56
122	22	19
123	56	57
124	4	2
125	14	26
126	12	−16
127	40	−39
128	17	−13
129	—	− 8
1,2,10	—	0
1,2,11	26	26
131	26	27
132	—	2
133	20	−21
134	61	−51
135	28	17
136	30	−22
137	37	22
138	47	47
139	19	−15
1,3,10	18	14
11$\bar{1}$	37	−32
11$\bar{2}$	61	66
11$\bar{3}$	52	48
11$\bar{4}$	41	−27
11$\bar{5}$	22	−22
11$\bar{6}$	—	− 5
11$\bar{7}$	36	−42
11$\bar{8}$	9	− 4
11$\bar{9}$	30	30
1,1,$\bar{10}$	28	−31
1,1,$\bar{11}$	—	2
12$\bar{1}$	62	−71
12$\bar{2}$	14	14
12$\bar{3}$	65	−72
12$\bar{4}$	36	−32
12$\bar{5}$	44	40
12$\bar{6}$	27	−26
12$\bar{7}$	29	−23
12$\bar{8}$	24	−21
12$\bar{9}$	—	3
1,2,$\bar{10}$	19	11
1,2,$\bar{11}$	35	28
13$\bar{1}$	9	8
13$\bar{2}$	28	26
13$\bar{3}$	2	− 3
13$\bar{4}$	61	−53
13$\bar{5}$	—	3
13$\bar{6}$	17	8
13$\bar{7}$	15	13
13$\bar{8}$	49	46
13$\bar{9}$	18	−13
1,3,$\bar{10}$	15	− 8
141	23	−27
142	—	3
143	22	19
144	35	34
145	40	35
146	10	− 3
147	35	−30
148	33	30
149	—	0
1,4,10	—	11
151	23	24
152	26	30
153	58	−56
154	24	29
155	17	−14
156	11	− 4
157	13	− 2
158	16	−14
159	32	−30
161	14	13
162	31	34
163	14	−11
164	8	− 3
165	35	−33
166	25	−30
167	23	18
168	—	− 6
171	4	− 8
172	32	−35
173	4	− 4
174	10	8
175	17	15
176	9	4
177	—	14
14$\bar{1}$	10	10
14$\bar{2}$	2	− 7
14$\bar{3}$	2	4
14$\bar{4}$	24	22
14$\bar{5}$	27	20
14$\bar{6}$	—	− 2
14$\bar{7}$	—	− 2
14$\bar{8}$	—	6
14$\bar{9}$	23	−19
1,4,$\bar{10}$	—	− 2
15$\bar{1}$	37	47
15$\bar{2}$	—	8
15$\bar{3}$	48	−48
15$\bar{4}$	29	19
15$\bar{5}$	27	22
15$\bar{6}$	5	0
15$\bar{7}$	39	36
15$\bar{8}$	24	−18
15$\bar{9}$	30	−24
16$\bar{1}$	10	11
16$\bar{2}$	4	8
16$\bar{3}$	14	−14
16$\bar{4}$	13	− 4
16$\bar{5}$	35	−28
16$\bar{6}$	37	−37
16$\bar{7}$	27	20
16$\bar{8}$	6	2
17$\bar{1}$	—	− 1
17$\bar{2}$	43	−45
17$\bar{3}$	14	−14
17$\bar{4}$	5	− 1
17$\bar{5}$	23	12
17$\bar{6}$	—	7
17$\bar{7}$	19	14
181	19	24
182	16	−17
183	9	6
184	—	5
185	24	−19
211	2	− 3
212	2	3
213	65	65
214	70	−74
215	11	−16
216	—	− 6
217	16	−23
218	30	33
219	29	34
2,1,10	11	11
2,1,11	12	−10
221	51	−44
222	22	−24
223	10	−12
224	—	1
225	29	21
226	20	22
227	39	−46
228	—	7
229	—	− 2
2,2,10	—	− 5
18$\bar{1}$	33	28
18$\bar{2}$	6	− 8
18$\bar{3}$	33	21
18$\bar{4}$	10	− 4
18$\bar{5}$	15	−16
21$\bar{1}$	53	−49
21$\bar{2}$	—	2
21$\bar{3}$	57	56
21$\bar{4}$	23	−34
21$\bar{5}$	—	6
21$\bar{6}$	9	5
21$\bar{7}$	30	−35
21$\bar{8}$	30	29
21$\bar{9}$	20	19
2,1,$\bar{10}$	6	8
2,1,$\bar{11}$	—	− 6
22$\bar{1}$	57	−56
22$\bar{2}$	10	−13
22$\bar{3}$	8	10
22$\bar{4}$	38	39
22$\bar{5}$	20	20
22$\bar{6}$	33	34
22$\bar{7}$	42	−42
22$\bar{8}$	—	3
22$\bar{9}$	18	−21
2,2,$\bar{10}$	16	−16
231	—	− 2
232	66	66
233	—	− 3
234	12	11

Table 2 (*cont.*)

hkl	F_o	F_c
235	11	−11
236	18	15
237	—	0
238	21	22
239	20	−17
2,3,10	31	−30
241	—	− 5
242	37	33
243	7	− 7
244	17	14
245	—	9
246	36	−37
247	—	− 8
248	—	− 8
249	—	2
251	—	− 9
252	31	−29
253	60	−67
254	12	−14
255	40	38
256	10	−12
257	39	33
258	—	10
259	24	−22
261	14	18
262	8	− 6
263	—	5
264	14	14
265	—	− 8
266	8	4
267	15	14
268	19	18
$23\bar{1}$	32	33
$23\bar{2}$	74	72
$23\bar{3}$	11	− 9
$23\bar{4}$	14	14
$23\bar{5}$	—	− 6
$23\bar{6}$	9	−11
$23\bar{7}$	16	17
$23\bar{8}$	14	12
$23\bar{9}$	15	− 9
$2,3,\bar{1}0$	19	−17
$24\bar{1}$	28	−28
$24\bar{2}$	22	23
$24\bar{3}$	21	−20
$24\bar{4}$	—	0
$24\bar{5}$	15	26
$24\bar{6}$	52	−51
$24\bar{7}$	—	−14
$24\bar{8}$	—	2
$24\bar{9}$	—	6
$25\bar{1}$	13	10
$25\bar{2}$	36	−38
$25\bar{3}$	57	−56
$25\bar{4}$	—	− 6
$25\bar{5}$	—	5
$25\bar{6}$	—	− 2
$25\bar{7}$	30	29
$25\bar{8}$	15	15
$25\bar{9}$	20	−17
$26\bar{1}$	32	29
$26\bar{2}$	23	18
$26\bar{3}$	18	24
$26\bar{4}$	—	13
$26\bar{5}$	—	−10
$26\bar{6}$	9	1
$26\bar{7}$	—	2
$26\bar{8}$	—	8
271	18	21
272	15	−15
273	14	−13
274	24	26
275	—	− 1
276	—	6
281	21	20
282	—	− 1
283	—	− 7
284	—	−13
311	10	− 6
312	37	37
313	20	17
314	17	12
315	16	−16
316	22	16
317	21	−31
318	18	16
319	9	12
3,1,10	39	−36
321	45	−34
322	12	8
323	42	−38
324	—	−16
325	43	39
326	—	− 6
327	11	−11
328	18	−21
329	—	− 4
$27\bar{1}$	13	14
$27\bar{2}$	15	−14
$27\bar{3}$	14	−10
$27\bar{4}$	24	22
$27\bar{5}$	—	− 8
$27\bar{6}$	—	0
$28\bar{1}$	11	10
$28\bar{2}$	—	− 4
$28\bar{3}$	—	− 2
$28\bar{4}$	—	− 7
$31\bar{1}$	2	2
$31\bar{2}$	58	49
$31\bar{3}$	30	28
$31\bar{4}$	21	22
$31\bar{5}$	18	−16
$31\bar{6}$	22	−22
$31\bar{7}$	—	2
$31\bar{8}$	—	6
$31\bar{9}$	21	19
$3,1,\bar{1}0$	10	−14
$32\bar{1}$	28	−24
$32\bar{2}$	7	− 3
$32\bar{3}$	11	10
$32\bar{4}$	46	−42
$32\bar{5}$	41	36
$32\bar{6}$	13	−10
$32\bar{7}$	19	−12
$32\bar{8}$	—	8
$32\bar{9}$	12	−10
331	10	−14
332	—	6
333	20	−23
334	63	−62
335	14	11
336	8	− 9
337	10	8
338	18	−16
339	—	1
341	26	−24
342	—	11
343	9	− 7
344	—	6
345	13	16
346	15	−11
347	10	− 8
348	21	25
351	31	36
352	—	3
353	—	− 4
354	18	17
355	—	12
356	15	12
357	12	13
361	26	21
362	31	28
363	—	− 5
364	19	16
365	17	−19
366	39	−43
$33\bar{1}$	—	3
$33\bar{2}$	11	− 3
$33\bar{3}$	27	−24
$33\bar{4}$	35	−36
$33\bar{5}$	18	16
$33\bar{6}$	—	−11
$33\bar{7}$	—	5
$33\bar{8}$	46	46
$33\bar{9}$	—	− 7
$34\bar{1}$	22	−22
$34\bar{2}$	14	9
$34\bar{3}$	12	8
$34\bar{4}$	62	58
$34\bar{5}$	—	13
$34\bar{6}$	—	− 6
$34\bar{7}$	29	−26
$34\bar{8}$	—	2
$35\bar{1}$	11	13
$35\bar{2}$	22	25
$35\bar{3}$	24	−24
$35\bar{4}$	—	10
$35\bar{5}$	—	− 7
$35\bar{6}$	—	− 4
$35\bar{7}$	—	− 1
$36\bar{1}$	—	6
$36\bar{2}$	—	4
$36\bar{3}$	—	− 6
$36\bar{4}$	15	18
$36\bar{5}$	21	−14
$36\bar{6}$	23	−31
371	15	−14
372	31	−30
373	9	− 8
374	13	14

Table 2 (*cont.*)

hkl	F_o	F_c	*hkl*	F_o	F_c	*hkl*	F_o	F_c
411	26	−23	$42\bar{1}$	8	− 6	525	16	18
412	16	8	$42\bar{2}$	8	2			
413	13	18	$42\bar{3}$	35	−24	531	—	− 2
414	43	−30	$42\bar{4}$	8	6	532	20	18
415	20	−16	$42\bar{5}$	41	36	533	—	− 9
416	29	−22	$42\bar{6}$	18	21	534	39	−41
417	10	− 5	$42\bar{7}$	16	−18	535	—	1
418	15	15						
			$43\bar{1}$	—	7	$45\bar{1}$	34	28
421	33	−29	$43\bar{2}$	52	51	$45\bar{2}$	23	−20
422	27	−26	$43\bar{3}$	21	−14	$45\bar{3}$	22	−16
423	33	33	$43\bar{4}$	33	−24	$45\bar{4}$	—	− 8
424	—	2	$43\bar{5}$	14	− 9	$45\bar{5}$	18	16
425	19	27	$43\bar{6}$	19	−23			
426	29	29	$43\bar{7}$	—	1	$46\bar{1}$	26	16
427	20	−20				$46\bar{2}$	—	0
			$44\bar{1}$	—	− 5	$46\bar{3}$	10	10
431	27	22	$44\bar{2}$	—	2	$46\bar{4}$	33	30
432	37	32	$44\bar{3}$	11	− 8			
433	—	− 9	$44\bar{4}$	—	− 5	$51\bar{1}$	29	−29
434	—	− 8	$44\bar{5}$	12	12	$51\bar{2}$	52	44
435	14	13	$44\bar{6}$	31	−29	$51\bar{3}$	18	14
436	—	− 1	$44\bar{7}$	17	9	$51\bar{4}$	17	−11
437	—	2				$51\bar{5}$	7	− 1
			451	—	0	$51\bar{6}$	19	−20
441	26	−24	452	—	0			
442	37	29	453	32	−28	$52\bar{1}$	29	−28
443	—	0	454	17	−16	$52\bar{2}$	5	− 6
444	13	9	455	16	12	$52\bar{3}$	12	−14
445	—	7				$52\bar{4}$	—	−13
446	39	−41	461	26	23	$52\bar{5}$	21	18
447	17	−18	462	—	− 2			
			463	—	4	$53\bar{1}$	20	9
$37\bar{1}$	20	−16	464	—	2	$53\bar{2}$	16	16
$37\bar{2}$	38	−40				$53\bar{3}$	—	5
$37\bar{3}$	11	7	511	—	1	$53\bar{4}$	—	−15
$37\bar{4}$	13	15	512	19	17	$53\bar{5}$	—	4
			513	33	27			
$41\bar{1}$	22	−22	514	19	− 9	541	—	− 4
$41\bar{2}$	14	−10	515	16	−13	542	—	− 5
$41\bar{3}$	21	22	516	13	12	543	—	13
$41\bar{4}$	51	−38						
$41\bar{5}$	—	0	521	27	−25	$54\bar{1}$	—	2
$41\bar{6}$	11	4	522	18	18	$54\bar{2}$	—	6
$41\bar{7}$	18	−18	523	—	12	$54\bar{3}$	—	− 2
$41\bar{8}$	43	38	524	—	4			

perature factor $\exp[-B(\sin\theta/\lambda)^2]$ with $B = 0{\cdot}5$ Å^2.

The two-dimensional Fourier maps of electron density are given in Fig. 2. Fig. 3 shows the result of the linear three-dimensional synthesis. The coordinates of atoms finally determined are given in Table 1. We give in Table 2 the F's calculated on the basis of these parameters, compared with those experimentally determined. (The relative intensities were made comparable with those calculated by multiplying by a proportionality factor that minimized the sum of a certain number of the differences, $F_o - F_c$). The reliability number, $R = \Sigma||F_o| - |F_c|| \div \Sigma|F_o|$, is 0·22 for all the reflexions observed.

The coordinates of calcium, silicon and boron atoms are considered accurate to within the experimental error of 0·01 Å and those oxygen atoms and OH groups to within 0·03 Å. The x coordinates of boron atoms and OH groups may probably be accurate to within 0·005 Å.

Description of the structure

The structure of datolite is illustrated in Fig. 4 (cf. Fig. 2).

Datolite is an orthosilicate containing separate SiO_4 groups. However, the structure may be conveniently described as superimposed complex sheets of linked oxygen and O–OH tetrahedra around silicon and boron atoms respectively.* In building up the sheet an Si–O and a B–O–OH tetrahedron alternate and form a ring of four tetrahedra on the one hand and one of eight tetrahedra on the other (Fig. 5). This mode of tetrahedral linkage is broadly the same with those found in apophyllite and other silicate minerals. The sheets are extended indefinitely parallel to (100) and

* The x coordinate of boron atom (0·600) reveals that it is almost at the centre of the O–OH tetrahedron ($x = 0{\cdot}58$). It would have $x = 0{\cdot}69$ if it were instead at the centre of the oxygen triangle.

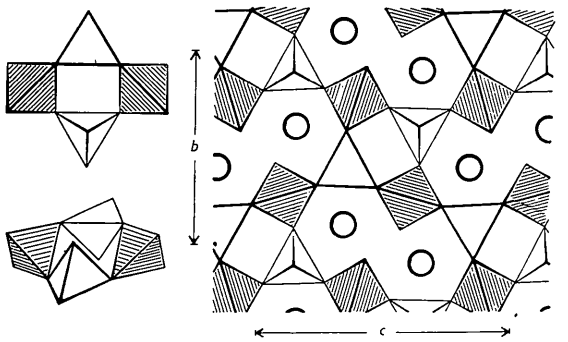

Fig. 5. The structure of datolite as linked tetrahedra of O and O–OH that make up a sheet (seen from the direction of the *a* axis). Ca atoms are shown by circles. SiO_4 tetrahedra are shaded and BO_3OH tetrahedra not shaded. Rings of four tetrahedra are singled out and drawn in projection and in perspective so as to make the reading of the figure easier.

held solidly together by calcium atoms which are in the middle of six oxygen atoms and two OH groups.

The balance of valency in the structure is illustrated in Fig. 6(*a*). The interatomic distances are given in Table 3.

Table 3. *Interatomic distances*

Atom	Neighbour	Distance (Å)	Atom	Neighbour	Distance (Å)
Si	O(1)	1·52	Ca	O(1)′	2·31
	O(2)*	1·66		O(1)*	2·30
	O(3)	1·69		O(2)	2·39
	O(4)	1·64		O(3)	2·55
B	O(2)	1·45		O(3)*	2·59
	O(3)	1·44		O(4)	2·49
	O(4)′	1·47		OH	2·71
	OH	1·56		OH*	2·59

O–O–OH distances in Å: O(1)–O(2)* 2·71, O(1)–O(3) 2·77, O(1)–O(4) 2·55, O(2)–O(3)′ 2·60, O(2)–O(4)″ 2·62, O(3)–O(4) 2·70, O(2)–O(3) 2·41, O(2)–O(4)′ 2·37, O(2)–OH 2·49, O(3)–O(4)′ 2·43, O(3)–OH 2·52, O(4)–OH 2·35.

* Atom of the neighbouring cell.
′, ″ Equivalent atoms.

The structure of datolite has apparently no relationship to that of euclase (Biscoe & Warren, 1933). It is to be noted that datolite has no conspicuous cleavage in spite of its sheet-like arrangement of atoms.

APPENDIX

On the structure of gadolinite

The structure of gadolinite may be derived from that of datolite simply by replacing calcium by yttrium, boron by beryllium and OH by oxygen and placing in addition iron at 0, 0, 0; 0, ½, ½. The balance of bonds will then be as perfectly maintained as in datolite (Fig. 6(*b*)). With these changes the coordinates of atoms given in Table 1 for datolite are applicable to gadolinite to the first approximation. The general agreement between F_c's and F_o's (obtained from powder photographs, Table 4) supports this view.

Table 4. *Powder photograph of gadolinite (from Otomé, Japan)*

Cu $K\alpha$ ($\lambda = 1{\cdot}54$ Å). Camera radius 28·63 mm. $Q_o = 4\sin^2\theta/\lambda^2$. $Q_c = h^2a^2 + k^2b^2 + l^2c^2 + 2lhca\cos\beta$. $a = 4{\cdot}71 \pm 0{\cdot}01$, $b = 7{\cdot}52 \pm 0{\cdot}01$, $c = 9{\cdot}89 \pm 0{\cdot}01$ Å ($\lambda = 1{\cdot}54$ Å), $\beta = 90°\ 33'$ (morphological, Dana (1900), p. 509). C_{2h}^5–$P2_1/c$. $Z = 2$ ($Fe_2Y_2Be_2Si_2O_{10}$). Intensities estimated visually.

hkl	Q_o	Q_c	I_o	$\frac{1}{4}F_c$
011	—	0·028	—	− 0·6
002	—	0·041	—	0·2
100	0·045	0·045	*w*	11·0
012	—	0·059	—	7·7
110	—	0·063	—	1·1
020	0·072	0·071	*vw*	3·0
11$\bar{1}$		0·073		− 6·0
111		0·073		− 8·5
021	0·083	0·081	*w*	−14·9
10$\bar{2}$	—	0·086	—	− 0·5
102	—	0·086	—	− 8·1
11$\bar{2}$	0·104	0·104	*s*	22·1
112		0·104		22·1
013	0·110	0·110	*w*	20·1
022	—	0·112	—	− 2·4
120	0·117	0·116	*w*	26·8
12$\bar{1}$	0·128	0·126	*s*	−29·4
121		0·126		−26·4
11$\bar{3}$	0·155	0·155	*s*	31·4
113		0·155		35·5
12$\bar{2}$		0·157		10·5
122		0·157		11·4
023	—	0·163	—	0·1
004	—	0·163	—	− 6·7
031	0·170	0·169	*vw*	15·6
200	0·182	0·180	*m*	11·2
014		0·181		−17·5

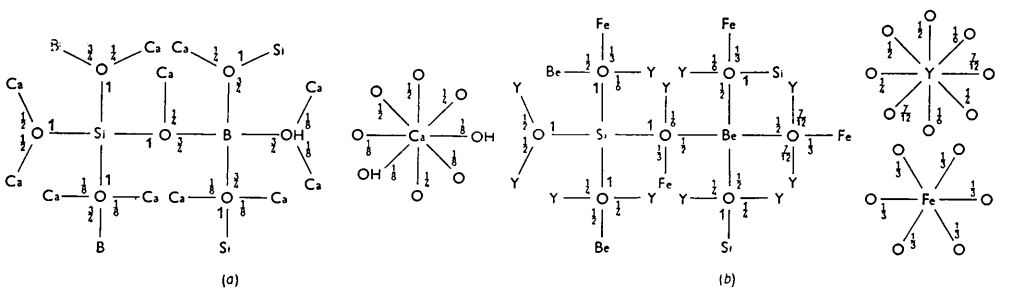

Fig. 6. Balance of bonds in (*a*) datolite and (*b*) gadolinite.

References

BISCOE, J. & WARREN, B. E. (1933). *Z. Krystallogr.* **86**, 292.
BRAGG, W. L. (1937). *The Atomic Structure of Minerals.* Ithaca: Cornell University Press.
DANA, E. S. (1900). *A System of Mineralogy*, 6th Ed. New York: Wiley.
GOSSNER, B. & MUSSGNUG, F. (1929). *Z. Krystallogr.* **70**, 171.

Acta Cryst. (1953). **6**, 32

The Structure of the Free Radical di-*p*-Anisyl Nitric Oxide

BY A. W. HANSON

Physics Department, College of Technology, Manchester 1, *England*

(*Received* 18 *July* 1952)

The unit cell of di-*p*-anisyl nitric oxide is orthorhombic, with $a = 7.33 \pm 0.04$, $b = 26.8 \pm 0.1$, $c = 6.25 \pm 0.03$ Å. The space group is *Aba*2, and in the unit cell there are four molecules, each lying on a twofold axis. The structure was solved by Fourier-transform methods, and the atomic positions, with bond lengths and angles, were found from the (100) and (001) Fourier projections.

Introduction

Di-*p*-anisyl nitric oxide is believed to be the first of the class of substances known as free radicals to be investigated by X-ray methods. This compound is quite stable, and the investigation, which depended largely on Fourier-transform methods, has presented no unusual difficulties.

Unit cell and space group

The sample supplied consisted of a mass of lath-like, red transparent crystals, from which it was not difficult to select single crystals suitable for X-ray examination. The unit cell was shown by oscillation photographs to be orthorhombic, and the unit-cell dimensions were found by considering the higher order $h00$, $0k0$ and $00l$ reflexions on *a*- and *c*-axis Weissenberg photographs. The results were:

$$a = 7{\cdot}33 \pm 0{\cdot}04,\ b = 26{\cdot}8 \pm 0{\cdot}1,\ c = 6{\cdot}25 \pm 0{\cdot}03 \text{ Å}.$$

A higher degree of accuracy is not claimed, since no allowance was made for film shrinkage.

The measured density of the sample was $1{\cdot}33 \pm 0{\cdot}01$ g.cm.$^{-3}$, and the calculated density, corresponding to four molecules in the unit cell, was $1{\cdot}32 \pm 0{\cdot}02$ g.cm.$^{-3}$.

The systematic absences were found to be: hkl for $k+l$ odd, $0kl$ for k odd or l odd, $h0l$ for h odd or l odd. These indicated the space group *Aba*2 or *Abam*; packing considerations soon showed that the second of these was improbable, and the space group was assumed to be *Aba*2.

Determination of the structure

The X-ray intensities of the $hk0$ and $0kl$ zones were estimated by visual comparison of each Weissenberg spot with a density wedge on similar film. The structure amplitudes were derived by using the usual trigonometrical factor; since the absorption coefficient of the substance was small, it was felt that further corrections were unnecessary.

The (100) projection, which showed the molecule roughly in plan, was solved by the Fourier-transform methods of Lipson & Taylor (1951). The problem was simplified by the fact that the space group *Aba*2 has eight general positions, so that the four molecules were known to lie on twofold axes. In this projection, moreover, only one molecule had to be considered.

The projection was non-centrosymmetrical, and approximate phase angles were determined in a way which will be described in a subsequent paper on optical diffraction methods. The Fourier plot corresponding to these phase angles resolved every atom, and the projection was refined in the usual way by means of successive Fourier syntheses. This process was carried only as far as the fifth synthesis, as it then appeared that the suggested changes were becoming aimless. The (001) projection, which was centrosymmetrical, was then solved almost immediately by conventional methods.

Discussion of the structure

In Table 1 are given the atomic positions consistent with both projections, while in Tables 2 and 3 are compared the observed and calculated structure factors for the $0kl$ and $hk0$ zones. All the structure-factor calculations were carried out by the method of Beevers & Lipson (1952), using Fourier strips. The factor of agreement $R = \Sigma||F_o|-|F_c|| \div \Sigma|F_o|$ is 0·15 for the $0kl$ zone, and 0·19 for the $hk0$ zone, although, if accidental absences in the zone are not considered,